Title	Galanin inhibits calcium channels via Galpha(i)-protein mediated by GalR1 in rat nucleus tractus solitarius
Author(s) Alternative	Endoh, T; Sato, D; Wada, Y; Shibukawa, Y; Ishihara, K; Hashimoto, S; Yoshinari, M; Matsuzaka, K; Tazaki, M; Inoue, T
Journal	Brain Research, 1229(): 37-46
URL	http://hdl.handle.net/10130/574
Right	

Research Report (BRES-D-08-00372R1) Re-Revised Version

Galanin inhibits calcium channels via $G\alpha_i$-protein mediated by GalR1 in rat nucleus tractus solitarius

Takayuki Endoh*, Daisuke Sato, Yoshiyuki Wada, Yoshiyuki Shibukawa, Kazuyuki Ishihara, Sadamitsu Hashimoto, Masao Yoshinari, Kenichi Matsuzaka, Masakazu Tazaki and Takashi Inoue

Oral Health Science Center HRC7, Tokyo Dental College,

1-2-2 Masago, Mihama-ku, Chiba 261-8502, Japan

*Corresponding author. Fax: +81 43 270 3771

E-mail address: tendoh@tdc.ac.jp (T. Endoh)

29 pages, 6 figures and figure legends

Keywords: Nucleus tractus solitarius; Galanin; Calcium channel current; Electrophysiology

ABSTRACT

Galanin (GAL), a 29-amino-acid neuropeptide, is involved in various neuronal functions, including the regulation of food intake, hormone secretion and central cardiovascular regulation. The nucleus tractus solitarius (NTS) is known to plays a major role in the regulation of cardiovascular, respiratory, gustatory, hepatic and swallowing functions. Voltage-dependent Ca^{2+} channels (VDCCs) serve as crucial mediators of membrane excitability and Ca^{2+}-dependent functions such as neurotransmitter release, enzyme activity and gene expression. The purpose of this study was to investigate the effects of GAL on VDCCs currents (I_{Ca}) carried by Ba^{2+} (I_{Ba}) in the NTS using patch-clamp recording methods. An application of M617 (GalR1 specific agonist), AR-M961 (GAL receptor GalR 1/2 agonist) and GAL caused inhibition of N- and P/Q-types I_{Ba}. M617, GAL, and AR-M961 caused inhibition of I_{Ba} in a concentration-dependent manner, with IC_{50}'s of 678 nM, 325 nM and 573 nM, respectively. This inhibition was relieved, albeit incompletely, by a depolarizing prepulse. Pretreatment with M35 (GalR non-specific antagonist) attenuated the M617-induced inhibition of I_{Ba}. Intracellular dialysis of the $G\alpha_i$-protein antibody also attenuated the Gal-induced inhibition of I_{Ba}. These results indicate that GAL inhibits N- and P/Q-types VDCCs via $G\alpha_i$ -protein $\beta\gamma$ subunits

mediated by GalR1 in NTS.

1. Introduction

Galanin (GAL), a 29-amino-acid neuropeptide, is widely distributed throughout the central nervous system (Waters and Krause, 2000). GAL is involved in a variety of functions, such as learning and memory, pain control, food intake, neuroendocrine control, and central cardiovascular regulation (Crawley, 1996; Wrenn and Crawley, 2001; Wynick et al., 2001; Narvaez et al., 1994).

The nucleus tractus solitarius (NTS) is known to plays a major role in the regulation of cardiovascular, respiratory, gustatory, hepatic and swallowing functions (Lawrence and Jarrott, 1996). In addition, caudal NTS is believed to belong to the swallowing pattern generators (Jean, 2001), whereas the rostal NTS is part of the taste pathways. The NTS appears not to be a simple 'relay' nucleus, rather it performs complex integration of information from multiple synaptic inputs of both peripheral and central origins (Paton, 1999).

Voltage-dependent Ca^{2+} channels (VDCCs) serve as crucial mediators of membrane excitability and Ca^{2+}-dependent functions such as neurotransmitter release, enzyme

activity and gene expression (Tsien et al., 1988; Sheng and Greenberg, 1990).

GAL is present in the NTS where it is costored in catecholaminergic cells being coreleased with adrenaline or noradrenaline (Melander et al., 1986) and its role on central cardiovascular regulation it has been clearly established (Diaz-Cabiale et al., 2005; Harfstrand et al., 1987). In addition, it has been demonstrated that GAL act as a neurotransmitter in the NTS (Tan et al., 2004). Three GAL receptors, GalR1, GalR2 and GalR3, have currently been cloned, and they are all G-protein-coupled receptors (GPCRs) (Habert-Ortoli et al., 1994; Branchek et al., 2000).

However, the effect of GAL on VDCCs in NTS has not yet been clarified, and little is known about signal transduction pathways in NTS. Consequently, it is the purpose of this study to investigate the effects of GAL on VDCCs currents (I_{Ca}) carried by Ba^{2+} (I_{Ba}) in NTS.

2. Results

2.1. GAL-induced inhibition of I_{Ba}

Representative examples of superimposed I_{Ba} traces in the absence and presence of 10

μM GAL are shown in Fig. 1. I_{Ba} was evoked every 20 sec with a 100 msec depolarizing voltage step to 0 mV from a holding potential of −80 mV. As shown in Fig. 1, application of GAL (in 30 of 48 neurons) rapidly and reversibly inhibits I_{Ba}. To investigate the voltage dependency of inhibition of I_{Ba} by GAL, we used a double-pulse voltage protocol as shown in Fig. 1A. As shown in Fig. 1A and B, the application of a strong depolarizing voltage prepulse attenuated GAL-induced inhibition of I_{Ba}.

The current-voltage relationships for I_{Ba} in the absence and presence of 10 μM GAL are shown in Fig. 1C. From a holding potential of −80 mV, the I_{Ba} was activated after −30 mV with a peak current amplitude at 0 mV.

2.2. GalR agonists-induced inhibition of I_{Ba}

In the next series of experiments, we investigated the effects of various GalR agonists on I_{Ba}.

GAL binds GalR1 with similar affinity to GalR2 (Ohtaki et al., 1999). Galanin-like peptide (GALP) is a 60-amino-acid neuropeptide, expressed in the hypothalamus and discrete areas of brain, which preferentially binds to GalR2 (Langel and Bartfai, 1998). To further examine which GalR were involved the GAL-induced inhibition of I_{Ba},

AR-M961 (GalR 1/2 agonist), AR-M1896 (GalR2 agonist) and M617 (galanin(1-13)-Gln^{14}-bradykinin(2-9)amide, GalR1 specific agonist, Lundstrom et al., 2005) were applied. As shown in Fig. 2 A and B, GALP (n＝5) did not modulate I_{Ba}. In contrast, AR-M961 (in 23 of 42 neurons) inhibited I_{Ba}. As shown in Fig. 2 C and D, AR-M1896 (n＝4) did not modulate I_{Ba}. In contrast, M617 (in 95 of 153 neurons) inhibited I_{Ba}.

These results indicate that GalR1, but not GalR2, is linked to inhibition of the I_{Ba} in NTS.

2.3. Dose dependence of GalR agonists-induced inhibition of I_{Ba}

The dose-response relations in the GalR agonists-induced inhibition of I_{Ba} is shown in Fig. 3. For the generation of the concentration-response curve, GalR agonists concentrations were applied randomly, and not all concentrations in a single neuron were tested. Fig. 3 shows that progressive increases in GalR agonists concentration resulted in progressively greater inhibition of I_{Ba}. M617 (GalR1 specific agonist), GAL, and AR-M961 (GalR1/2 agonist) caused inhibition of I_{Ba} in a concentration-dependent manner.

The lowest concentration of the agonists used 10 nM inhibited I_{Ba} by 2.2 ± 2.0% (n＝4), in these experiments a maximal concentration of M617 (10 μM) inhibited I_{Ba} by 25.8 ± 2.8% (n＝5). Inhibition in I_{Ba} was found at all concentrations greater than 10 nM. The effect was maximal at concentrations in excess of 10 μM, and the mean inhibition in I_{Ba} at this concentration was 25.8 ± 2.8% (n＝5). From these data the IC_{50} value for M617, GAL and AR-M961 on I_{Ba} was 678 nM, 325 nM and 573 nM, respectively.

Galanin(2-11) (GalR 2/3 agonist), AR-M1896 (GalR2 agonist) and GALP (GalR2 agonist) did not inhibit I_{Ba}. These pharmacological profile indicate that only GalR1 couples with VDCCs in NTS.

2.4. Pharmacological characterization of GalR agonists-induced inhibition of I_{Ba}

In the next series of experiments, we analyzed the effects of GalR agonists on I_{Ba} in neurons treated with specific GalR antagonists. In this experiment, specific antagonists M35 (non-selective GalR antagonist) and M871 (galanin-(2-13)-Glu-His-$(Pro)_3$-$(Ala-Leu)_2$-Ala-amide, selective GalR2 antagonist, Sollenberg et al., 2006) were applied prior to the M617. Treatment with M35 (10 μM

for 3 min after assuming the whole-cell configuration) attenuated the M617-induced inhibition of I_{Ba}. In contrast, treatment with M871 (10 μM for 3 min after assuming the whole-cell configuration) did not attenuate the M617-induced inhibition of I_{Ba}. These results indicated that M617-induced inhibition of I_{Ba} was mediated by GalR1 in NTS.

2.5. Characterization of G-protein subtypes in GalR agonists-induced inhibition of I_{Ba}

The G-protein is heterotrimeric molecules with α, β and γ subunits. The α subunit can be classified into families, $G\alpha_{i/o}$, $G\alpha_{s}$, or $G\alpha_{q/11}$. To characterize the G-protein subtypes in M617-induced inhibition of I_{Ba}, specific antibody raised against the $G\alpha_{i}$-, $G\alpha_{s}$- and $G\alpha_{q/11}$-protein were used. Experiments were performed using a solution in a pipette containing each G-protein antibody. In these experiments, the G-protein antibody (1:50 dilution; the final concentration was approximately 0.5 mg/ml) was dissolved in the internal solution. The tip of the recording pipette was filled with the standard internal solution, and the pipette was then backfilled with solution which containing the G-protein antibody. In order to obtain the effect of antibody, M617 were applied 7 min after assuming the whole-cell configuration.

As shown in Fig. 4, intracellular dialysis of the $G\alpha_i$-protein antibody attenuated the M617-induced inhibition I_{Ba}. In contrast, intracellular dialysis of boiled $G\alpha_i$-protein antibody (90 ℃ for 30 min), $G\alpha_s$- and $G\alpha_{q/11}$-proteins antibodies did not attenuate the M617-induced inhibition of I_{Ba}. These results suggest that the $G\alpha_i$-protein are involved in the M617-induced inhibition of I_{Ba} in NTS but $G\alpha_s$- and $G\alpha_{q/11}$-proteins are not.

2.6. Characterization of VDCCs subtypes in GalR agonists-induced inhibition of I_{Ba}

Several studies have defined pharmacological distinct high voltage-activated (HVA) VDCCs on neuronal cell bodies, such as L-, N-, P-, Q- and R-type VDCCs. In this study, specific VDCCs blockers were used to isolate each VDCCs current component. We previously demonstrated that mean percentages of L-type I_{Ba} components (I_{Ba-L}), N-type I_{Ba} components (I_{Ba-N}), P/Q-type I_{Ba} components ($I_{Ba-P/Q}$) and R-type I_{Ba} components (I_{Ba-R}) of total I_{Ba} was 42.2 ± 3.8%, 28.4 ± 3.4%, 19.3 ± 3.2% and 10.1 ± 1.4%, respectively in NTS (Endoh, 2006). Therefore, it was investigated about which types of the VDCCs were inhibited by M617. The effect of M617 on the I_{Ba-L} was investigated using a neuron treated with ω-conotoxin GVIA (ω-CgTx GVIA, N-type VDCCs blocker, 1 μM) and ω-agatoxin IVA (ω-Aga IVA, P/Q-types VDCCs blocker, 1 μM). The effect

of M617 on the I_{Ba-N} was investigated using a neuron treated with Nifedipine (Nif, L-type VDCCs blocker, 10 μM) and ω-Aga IVA (1 μM). The effect of M617 on the $I_{Ba-P/Q}$ was investigated using a neuron treated with Nif (10 μM) and ω-CgTx GVIA (1 μM). The effect of M617 on the I_{Ba-R} was investigated using a neuron treated with Nif (10 μM), ω-CgTx GVIA (1 μM) and ω-Aga IVA (1 μM).

Each of the I_{Ba} components and the percentage of the inhibition by M617 are summarized in Fig. 5e. The percentages of each type of current illustrated were constructed by mixture of both previous study (Endoh, 2006) and de novo data for the present study. The current-voltage relationships for distinct I_{Ba} components in the absence and presence of 10 μM M617 are shown in Fig. 6. Results shown in Figs. 5 and 6 demonstrate that M617 inhibited I_{Ba-N} and $I_{Ba-P/Q}$ in NTS.

3. Discussion

This study has shown that GAL inhibits N- and P/Q-types VDCCs via $G\alpha_i$-protein mediated by GalR1 in NTS.

Several demonstrations suggest that GAL modulate VDCCs in other neurons. For example, GAL modulate VDCCs in dorsal root ganglion (DRG) neurons (Kerekes et al.,

2003), in hypothalamic neurons (Simen et al., 2001) and in mudpuppy cardiac ganglia (Parsons et al., 1998).

As mentioned above, three GAL receptors have been cloned: GalR1, GalR2 and GalR3. These GalR are coupled to distinct signaling cascades. Both GalR1 and GalR3 signal via $G\alpha_i$-protein and decrease cyclic AMP levels by inhibiting adenylate cyclase (Smith et al., 1997). On the other hand, the main pathway downstream from GalR2 is through coupling to $G\alpha_{q/11}$-protein and activates phospholipase C (PLC) to increase inositol triphosphate accumulation and the increase of intracellular Ca^{2+} (Wang et al., 1998; Lundstrom et al., 2005); this would presumably stimulate neuronal activity and neurotransmitter release. In this study, AR-M1896 (GalR2 agonist) did not modulate I_{Ba} in NTS. Similar results were observed in hypothalamic neurons (Simen et al., 2001). They have demonstrated that GAL inhibits I_{Ba}, but [D-Trp^2] galanin (GalR2 agonist) did not in hypothalamic neurons. In contrast, both GAL and AR-M1896 (GalR2 agonist) facilitates I_{Ca} in DRG (Kerekes et al., 2003).

Moreover, we found that I_{Ba} inhibition by GAL via $G\alpha_i$-protein. Intracellular dialysis of the $G\alpha_i$-protein antibody attenuated M617 (GalR1 agonist)-induced inhibition I_{Ba} in NTS (Fig. 4). Similar results were reported in mudpuppy cardiac ganglia (Parsons et al., 1998). They demonstrated that GAL-induced inhibition of I_{Ba} was attenuated by 24-30

hour pretreatment with pertussis toxin (PTX). Previously, several studies have demonstrated that PTX sensitive $G\alpha_i$-protein are involved in the endocrine (Amiranoff et al., 1988; Lagny-Pourmir et al., 1989) and neuromodulatory (Bartfai et al., 1992; Palazzi et al., 1991; Tsuda et al., 1992; Tyszkiewicz et al., 2008) action of GAL.

We also found that the effects of GAL were relieved, albeit incompletely, by a depolarizing prepulse (Fig. 1A). Such an effect is usually interpreted as an indication that VDCCs inhibition is mediated by a rapid membrane delimited pathway, possibly involving an interaction between the $G\alpha_i$-protein $\beta\gamma$ subunits with the VDCCs α_1-subunit (Zamponi et al., 1998). Herlitze et al. (1996) have been demonstrated that G-protein $\beta\gamma$ subunits can interact directly with N- and P/Q-types VDCCs to inhibit their activation.

In this study, the IC_{50} of M617 (GalR1 specific agonist), GAL, and AR-M961 (GalR1/2 agonist) were 678 nM, 325 nM and 573 nM, respectively, in NTS. IC_{50} values for GAL-induced modulation of I_{Ca} have been calculated in other tissues. In guinea-pig myenteric ganglion, (1.4 nM, Ren et al., 2001) and mudpuppy cardiac ganglia cells (0.4 nM, Parsons et al., 2000) it was found to be more than 100-fold more than potent than in NTS. The discrepancy observed in these studies carried out in different cell types may be due to cell-dependent differences in the regulation of membrane excitability.

It has been reported that GAL facilitates inwardly rectifying K (Kir) channels in CNS. Kir channels have been classified into four subfamilies: 1) IRK subfamily (IRK1-3), 2) GIRK subfamily, 3) ATP-dependent Kir subfamily, 4)ATP-sensitive Kir subfamily (Isomoto et al., 1997). Coupling of GalR1 to $G\alpha_i$-protein facilitates G-protein-mediated inward rectifier K^+ channels (GIRK) or ATP-sensitive K^+ channels, which in turn results in presynaptic inhibition of glutamatergic transmission (Mazarati et al., 2000; Counts et al., 2002; Lundstrom et al., 2005). In myenteric ganglion, GAL inhibits VDCCs and facilitates GIRK channels (Ren et al., 2001). If the GIRK channels are facilitated by GAL, so that neuronal activity may be suppressed. In this study, GIRK channels actions were masked, since the Ba^{2+} introduced for the measurements can block the GIRK channels. It is not clear what types of Kir channels are modulated by GAL in NTS. In normal state, both inhibition of VDCCs and facilitation of GIRK channels deduced to occur with GAL on NTS.

It has been demonstrated that microinjection of GAL into the NTS depressed baroreceptor reflex response (Shin et al., 1996). Chen et al. demonstrated that hypothalamic paraventricular nucleus (PVN) galaninergic projections to NTS suppress baroreceptor reflex respomses, giving evidence on the involvement of GAL in cardiovascular regulation (Chen et al., 1996). NTS neurons can be divided into two

groups, glutamatergic and GABAergic (Mifflin and Felder, 1990; Brooks et al., 1992). It can be considered that inhibition of VDCCs on glutamatergic neurons can decrease glutamate release and therefore a reduced baroreflex function. N-, P- and Q-types VDCCs are implicated in transmitter release in CNS (Reuter, 1996). In fact, several studies demonstrated that GAL reduced glutamate release in CNS (Kinney et al., 1998; Kozoriz et al., 2006).

Microinjection of GAL into the NTS stimulates feeding in rats (Koegler and Ritter, 1998; Koegler et al., 1999). Neurons responsive to both gustatory and lingual somatosensory stimuli have been identified in the NTS (Travers and Norgren, 1995). Therefore, GAL effects in NTS should be investigated in a further study.

4. Experimental Procedures

4.1. Cell preparation

The study was carried out according to "The guideline for the treatment of experimental animals in Tokyo Dental College". NTS neurons were prepared as described previously (Endoh, 2005). Briefly, young Wistar rats (7-18 days old) were decapitated and their

brains were quickly removed and submerged in ice cold artificial cerebrospinal fluid (aCSF) saturated with 95% O_2 and 5% CO_2 of the following composition (in mM): 126 NaCl, 26.2 $NaHCO_3$, 1 NaH_2PO_4, 3 KCl, 1.5 $MgSO_4$, 1.5 $CaCl_2$ and 30 glucose; pH 7.4. Thin transverse slices from brainstems, 400 μm in thickness, were prepared by a tissue slicer (DTK-1000; Dosaka EM Co., Ltd, Kyoto). After being sectioned, 3-5 slices obtained from a single brain were transferred to a holding chamber and stored in oxygenated aCSF at room temperature for at least 40 min before use. Slices were then transferred to a conical tube containing gently bubbled aCSF at 36 ℃ to which 1.8 U/ml dispase (grade Ⅰ; 0.75 ml/slice) was added. After 60 min incubation, slices were rinsed with enzyme-free aCSF. Under a dissecting microscope, the NTS region was micropunched and placed on a poly-l-lysine-coated coverslip. The cells were then dissociated by trituration using progressively smaller diameter pipettes and allowed to settle on a coverslip for 20 min.

4.2. Whole-cell patch-clamp recordings

Voltage-clamp recordings were conducted using the whole-cell configuration of the patch-clamp technique (Hamill et al., 1981). Fabricated recording pipettes (2-3 MΩ)

were filled with the internal solution of the following composition (in mM): 100 CsCl, 1 $MgCl_2$, 10 HEPES, 10 BAPTA, 3.6 MgATP, 14 $Tris_2$phosphocreatine (CP), 0.1 GTP, and 50 U/ml creatine phosphokinase (CPK). The pH was adjusted to 7.2 with CsOH. After the formation of a giga seal, in order to record I_{Ca} carried by Ba^{2+} (I_{Ba}), the external solution was replaced from aCSF solution to a solution containing the following (in mM): 151 tetraethylammonium (TEA) chloride, 5 $BaCl_2$, 1 $MgCl_2$, 10 HEPES and 10 glucose. The pH was adjusted to 7.4 with TEA-OH. Command voltage protocols were generated with a computer software pCLAMP version 8 (Axon Instruments, Union City, CA, U.S.A.) and transformed to an analogue signal using a DigiData 1200 interface (Axon Instruments, Union City, CA, U.S.A.). The command pulses were applied to cells through an L/M-EPC7 amplifier (HEKA Elektronik, Lambrecht, Germany). The currents were recorded with the amplifier and a computer software pCLAMP 8 acquisition system. Access resistance ($< 15\ M\Omega$) was determined by transient responses to voltage commands. Access resistance compensation was not used. To ascertain that no major changes in the access resistance had occurred during the recordings a 5 mV, 10 msec pulses were used before I_{Ba} was evoked.

4.3. Materials

GAL, ω-CgTx GVIA and ω-Aga IVA were purchased from Peptide Institute (Osaka, Japan). GALP, Galanin(2-11) and Nif were purchased from Sigma (Tokyo, Japan). AR-M961 and M35 were purchased from Wako Pure Chemical Industries (Osaka, Japan). AR-M1896, M617 and M871 were purchased from Tocris (Avonmouth, U.K.). Anti-Gα_i antibodies, anti-Gα_s antibodies and anti-G$\alpha_{q/11}$ antibodies were purchased from Upstate biotechnology (Lake Placid, NY, U.S.A.). Each antibodies were from rabbits immunized with a synthetic peptide corresponding to the COOH-terminal sequence of the human Gα_i, Gα_s and G$\alpha_{q/11}$, respectively.

4.4. Data analysis and statistics

All data analysis was performed using the pCLAMP 8.0 acquisition system. Values in text and figures are expressed as mean ± SEM. Statistical analysis was made by student *t*-test for comparisons between pairs of groups and by one-way analysis of variance (ANOVA) followed by Dunnett's test. Probability (p) values of less than 0.05 were considered significant.

Acknowledgements

This research was supported by Oral Health Science Center Grant HRC7 from Tokyo Dental College, and by a “High-Tech Research Center” Project for Private Universities: matching fund subsidy from MEXT (Ministry of Education, Culture, Sports, Science and Technology) of Japan and 2006-2010 (No.19592414).

REFERENCES

Amiranoff, B., Lorinet, A.-M., Lagny-Pourmir, I., Laburthe, M., 1988. Mechanism of galanin-inhibited insulin release. Occurrence of a pertussis-toxin-sensitive inhibition of adenylate cyclase. Eur. J. Biochem. 177, 147-152.

Bartfai, T., Fisone, G., Langel, U., 1992. Galanin and galanin antagonists: molecular and biochemical perspectives. Trends Pharmacol. Sci. 13, 312-317.

Branchek, T.A., Smith, K.E., Gerald, C., Walker, M.W., 2000. Galanin receptor subtypes. Trends Pharmacol. Sci. 21, 109-117.

Brooks, P.A., Glaum, S.R., Miller, R.J., Spyer, K.M., 1992. The actions of baclofen on neurons and synaptic transmission in the nucleus tractus solitarii of the rat in vitro. J. Physiol. 457, 115-129.

Chen, Y.L., Chan, S.H., Chan, J.Y., 1996. Participation of galanin in baroreflex inhibition of heart rate by hypothalamic PVN in rat. Am. J. Physiol. 271, H1823-H1828.

Counts, S.E., McGuire, S.O., Sortwell, C.E., Crawley, J.N., Collier, T.J., Mufson, E., 2002. Galanin inhibits tyrosine hydroxylase expression in midbrain dopaminergic neurons. J. Neurochem. 83, 442-451.

Crawley, J.N., 1996. Galanin-acetylcholine interactions: relevance to memory and Alzheimer's disease. Life Sci. 58, 2185-2199.

Diaz-Cabiale, Z., Parrado, C., Vela, C., Razani, H., Covenas, R., Fuxe, K., Narvaez, J.A., 2005. Role of galanin and galanin(1-15) on central cardiovascular control. Neuropeptides 39, 185-190.

Endoh, T., 2005. Involvement of Src tyrosine kinase and mitogen-activated protein kinase in the facilitation of calcium channels in rat nucleus tractus solitarius by angiotensin Ⅱ. J. Physiol. 568, 851-865.

Endoh, T., 2006. Pharmacological characterization of inhibitory effects of postsynaptic opioid- and cannabinoid-receptors on calcium currents in neonatal rat nucleus tractus

solitarius. Br. J. Pharmacol. 147, 391-401.

Habert-Ortoli, E., Amiranoff, B., Loquet, I., Laburthe, M., Mayaux, J.F., 1994. Molecular cloning of a functional human galanin receptor. Proc. Natl. Acad. Sci. USA 91, 9780-9783.

Hamill, O.P., Marty, A., Neher, E., Sakmann, B., Sigworth, F.J., 1981. Improved patch-clamp techniques for high-resolution current recording from cells and cell-free membrane patches. Pfugers. Arch. 391, 85-100.

Harfstrand, A., Fuxe, K., Melander, T., Hokfelt, T., Agnati, L.F., 1987. Evidence for a cardiovascular role of central galanin neurons, focus on interactions with a2-adrenergic and neuropeptide Y mechanisms. J. Cardiovasc. Pharmacol. 10, 199-204.

Herlitze, S., Garcia, D.E., Mackie, K., Hille, B., Scheuer, T., Catterall, W.A., 1996. Modulation of Ca^{2+} channels by G-protein $\beta\gamma$ subunits. Nature 380, 258-262.

Isomoto, S., Kondo, C., Kurachi, Y., 1997. Inwardly rectifying potassium channels: their

molecular heterogeneity and function. Jpn. J. Physiol. 47, 11-39.

Jean, A., 2001. Brain stem control of swallowing: neuronal network and cellular mechanisms. Physiol. Rev. 81, 929-969.

Kerekes, N., Mennicken, F, O'Donnell, D., Hokfelt, T., Hill, R.H., 2003. Galanin increases membrane excitability and enhances Ca^{2+} currents in adult, acutely dissociated dorsal root ganglion neurons. Eur. J. Neurosci. 18, 2957-2966.

Kinney, G.A., Emmerson, P.J., Miller, R.J., 1998. Galanin receptor-mediated inhibition of glutamate release in the arcuate nucleus of the hypothalamus. J. Neurosci. 18, 3489-3500.

Koegler, F.H., Ritter, S., 1998. Galanin injection into the nucleus of the solitary tract stimulates feeding in rats with lesions of the paraventricular nucleus of the hypothalamus. Physiol. Behav. 63, 521-527.

Koegler, F.H., York, D.A., Bray, G.A., 1999. The effects on feeding of galanin and M40

when injected into the nucleus of the solitary tract, the lateral parabrachial nucleus and the third ventricle. Physiol. Behav. 67, 259-267.

Kozoriz, M.G., Kuzmiski, J.B., Hirasawa, M., Pittman, Q.J., 2006. Galanin modulates neuronal and synaptic properties in the rat supraoptic nucleus in a use and state dependent manner. J. Neurophysiol. 96, 154-164.

Lagny-Pourmir, I., Amiranoff, B., Lorinet, A.M., Tatemoto, K., Laburthe, M., 1989. Characterization of galanin receptors in the insulin-secreting cell line Rin m 5F: evidence for coupling with a pertussis toxin-sensitive guanosine triphosphate regulatory protein. Endocrinology 124, 2635-2641.

Langel, U., Bartfai, T., 1998. Chemistry and molecular biology of galanin receptor ligands. Ann. NY Acad. Sci. 863, 86-93.

Lawrence, A., Jarrott, B., 1996. Neurochemical modulation of cardiovascular control in the nucleus tractus solitarius. Prog. Neurobiol. 48, 21-53.

Lundstrom, L., Elmquist, A., Bartfai, T., Langel, U., 2005. Galanin and its receptors in neurological disorders. Neuromol. Med. 7, 157-180.

Lundstrom, L., Sollenberg, U., Brewer A., Kouya, P.F., Zheng, K., Xu X.-J., Sheng, X., Robinson , J.K., Wiesenfeld-Hallin, Z., Xu, Z.-Q., Hokfelt, T., Bartfai, T., Langel, U., 2005. A galanin receptor subtype 1 specific agonist. Int. J. Peptide Res. Therapeutics 11, 17-27.

Mazarati, A.M., Hohmann, J.G., Bacon, A., Liu, H., Sankar, R., Steiner, R.A., Wynick, D., Wasterlain, C.G., 2000. Modulation of hippocampal excitability and seizures by galanin. J. Neurosci. 20, 6276-6281.

Melander, T., Hokfelt, T., Rokaeus, M., Cuello, A.C., Oertel, W.H., Verhofstad, A., Golstei, M., 1986. Coexistence of galanin-like immunoreactivity with cathecholamines, 5-hydroxy-tryptamine, Gaba and neuropeptides in the rat. J. Neurosci. 6, 3640-3654.

Mifflin, S.W., Felder, R.B., 1990. Synaptic mechanisms regulating cardiovascular afferent inputs to solitary tract nucleus. Am. J. Physiol. 28, H653-H661.

Narvaez, J.A., Diaz, Z., Aguirre, J.A., Gonzalez-Baron, S., Yanaihara, N., Fuxe, K., Hedlund, P.B., 1994. Intracisternally injected galanin-(1-15) modulates the cardiovascular responses of galanin-(1-29) and the 5-HT1A receptor agonist 8-OH-DPAT. Eur. J. Pharmacol. 257, 257-265.

Ohtaki, T., Kumano, S., Ishibashi, Y., Ogi, K., Matsui, H., Harada, M., Kitada, C., Kurokawa, T., Onda, H., Fujino, M., 1999. Isolation and cDNA cloning of a novel galanin-like peptide (GALP) from porcine hypothalamus. J. Biol. Chem. 274, 37041-37045.

Palazzi, E., Felinska, S., Zambelli, M., Fisone, G., Bartfai, T., Consolo, S., 1991. Galanin reduces carbachol stimulation of phosphoinositide in rat ventral hippocampus by lowering Ca^{2+} influx through voltage-sensitive Ca^{2+} channels. J. Neurochem. 56, 739-747.

Parsons, R.L., Mulvaney, J.M., Merriam, L.A., 1998. Galanin activates an inwardly rectifying potassium conductance and inhibits a voltage-dependent calcium

conductance in mudpuppy parasympathetic neurons. Ann. NY Acad. Sci. 863, 159-169.

Paton, J.F.R., 1999. The Sharpey-Schafer prize lecture. Nucleus tractus solitarii: integrating structures. Exp. Physiol. 84, 815-833.

Ren, J., Hu H.-Z., Starodub, A.M., Wood, J.D., 2001. Galanin suppresses calcium conductance and activates inwardly rectifying potassium channels in myenteric neurones from guinea-pig small intestine. Neurogastroenterol. Mot. 13, 247-254.

Reuter, H., 1996. Diversity and function of presynaptic calcium channels in the brain. Curr. Opin. Neurobiol. 6, 331-337.

Shin, C.-D., Chan, S.H.H., Chan, J.Y.H., 1996. Participation of endogenous galanin in the suppression of baroreceptor reflex response by locus coeruleus in the rat. Brain Res. 721, 76-82.

Sheng, M., Greenberg, M.E., 1990. The regulation and function of c-fos and other immediate early genes in the nervous system. Neuron 4, 477-485.

Simen, A.A., Lee, C.C., Simen, B.B., Bindokas, V.P., Miller, R.J., 2001. The C terminus of the Ca channel α1B subunit mediates selective inhibition by G-protein-coupled receptors. J. Neurosci. 21, 7587-7597.

Smith, K.E., Forray, C., Walker, M.W., Jones, K.A., Tamm, J.A., Bard, J., Branchek, T.A., Linemeyer, D.L., Gerald, C., 1997. Expression cloning of a rat hypothalamic galanin receptor coupled to phosphoinositide turnover. J. Biol. Chem. 39, 24612-24616.

Sollenberg, U.E., Lundstrom, L., Bartfai, T., Langel, U., 2006. M871 – a novel peptide antagonist selectively recognizing the galanin receptor type 2. Int. J. Peptide Res. Therapeutics 12, 115-119.

Tan, Z., Fogel, R., Jiang, C., Zhang, X., 2003. Galanin inhibits gut-related vagal neurons in rats. J. Neurophysiol. 91, 2330-2343.

Travers, S.P., Norgren, R., 1995. Organization of orosensory responses in the nucleus of the solitary tract of rat. J. Neurophysiol. 73, 2144-2162.

Tsien, R.W., Lipscombe, D., Madison, D.V., Bley, K.R., Fox, A.P., 1988. Multiple types of neuronal calcium channels and their selective modulation. Trends Neurosci. 11, 431-438.

Tsuda, K., Tsuda, S., Nishio, I., Masuyama, Y., Goldstein, M., 1992. Modulation of norepinephrine release by galanin in rat medulla oblongata. Hypertension 20, 361-366.

Tyszkiewicz, J.P., Fong T.M., Dong, Y., 2008. $GABA_B$ receptors are required for galanin modulation of membrane properties of neurons in the arcuate nucleus of rats. Brain Res. 1191, 63-68.

Verhofstad, A., Goldstei, M., 1986. Coexistence of galanin-like immunoreactivity with cathecholamines, 5-hydroxy-tryptamine, Gaba and neuropeptides in the rat. J. Neurosci. 6, 3640-3654.

Wang, S., Hashemi, T., Fried, S., Clemmons, A.L., Hawes, B.E., 1998. Differential intracellular signaling of the GalR1 and GalR2 galanin receptor subtypes. Biochemistry

37, 6711-6717.

Waters, S.M., Krause, J.E., 2000. Distribution of galanin-1, -2 and -3 receptor messenger RNAs in central and peripheral rat tissues. Neuroscience 95, 265-271.

Wrenn, C.C., Crawley, J.N., 2001. Pharmacological evidence supporting a role for galanin in cognition and affect. Prog. Neuro-Psychopharmacol. Biol. Psychiatry 25, 283-299.

Wynick, D., Thomson, S.W.W., McMahon, S.B., 2001. The role of galanin as a multi-functional neuropeptide in the nervous system. Curr. Opin. Pharmacol. 1, 73-77.

Zamponi, G.W., Snutch, T.P., 1998. Modulation of voltage-dependent calcium channels by G protein. Curr. Opin. Neurobiol. 8, 351-356.

Fig.1 GAL-induced inhibition of I_{Ba}. (A) Typical superimposed I_{Ba} traces recorded using a double-pulse voltage protocol at the times indicated in the time course graph B. Paired I_{Ba} were evoked from a holding potential of −80 mV by a 100 msec voltage step to 0 mV at 20 sec intervals. An intervening strong depolarizing prepulse (100 mV, 30 msec) ended 5 msec prior to the second I_{Ba} activation. (B) Typical time course of GAL-induced inhibition of I_{Ba}. GAL (10 μM) was bath-applied during the time indicated by the filled bar. (C) Current-voltage relations of I_{Ba} evoked by a series of voltage steps from a holding potential of −80 mV to test potentials between −80 and +40 mV in +10 mV increments in the absence (opened points) and presence (filled points) of 10 μM GAL. Values of I_{Ba} are the averages of five neurons.

Fig.2 Various GalR agonists-induced inhibition of I_{Ba}. (A) Typical superimposed I_{Ba} traces at the times indicated in the time course graph B. I_{Ba} were evoked from a holding potential of −80 mV by a 100 msec voltage step to 0 mV at 20 sec intervals. (B) Typical time course of GALP- and AR-M961-induced inhibition of I_{Ba}. GALP (Galanin-like peptide, 10 μM) and AR-M961 (GalR 1/2 agonist, 10 μM) were bath-applied during the time indicated by the filled bar. (C) Typical superimposed I_{Ba} traces at the times indicated in the time course graph D. I_{Ba} were evoked from a holding potential of −80 mV by a 100 msec voltage step to 0 mV at 20 sec intervals. (D) Typical time course of AR-M1896- and M617-induced facilitation of I_{Ba}. AR-M1896 (GalR2 agonist, 10 μM) and M617 (GalR1 agonist, 10 μM) were bath-applied during the time indicated by the filled bar.

Fig.3 Dose dependence of various GalR agonists. Concentration-response curves for I_{Ba} inhibition induced by M617 (■,GalR1 agonist), GAL (○, Galanin), AR-M961 (◇, GalR 1/2 agonist), Galanin(2-11) (◆, GalR 2/3 agonist), AR-M1896 (●, GalR2 agonist) and GALP (□, Galanin-like peptide). I_{Ba} were evoked from a holding potential of −80 mV by a 100 msec voltage step to 0 mV at 20 sec intervals. The inhibition (%) was normalized to that induced by each agonist at a maximal concentration. The curve was obtained from fitting to a single-site binding isotherm with least-squares nonlinear regression.

Fig.4 GalR1 agonist-induced inhibition of I_{Ba} under various conditions. (A) Typical superimposed I_{Ba} traces at the times indicated in the time course graph B. I_{Ba} were evoked from a holding potential of −80 mV by a 100 msec voltage step to 0 mV at 20 sec intervals. (B) Typical time course of M617-induced I_{Ba} inhibition in a neuron treated with M35 (non-selective GalR antagonist, 10 μM). M35 and M617 were bath-applied during the time indicated by the open and filled bars, respectively. (C) Summary of M617-induced inhibition of I_{Ba} under various conditions. I_{Ba} inhibition by 10 μM M617 in control (untreated neurons), after M35 (non-selective GalR antagonist), after M871 (GalR2 antagonist), intracellular dialysis with anti-$G\alpha_i$ antibody, intracellular dialysis with boiled anti-$G\alpha_i$ antibody, intracellular dialysis with anti-$G\alpha_s$ antibody and intracellular dialysis with anti-$G\alpha_{q/11}$ antibody. Numbers in parentheses indicate the number of neurons tested. *$p < 0.05$ compared with control.

Fig.5 GalR1 agonist-induced inhibition of distinct I_{Ba}. (A) Typical superimposed I_{Ba} traces recorded at the times indicated in the time course graph B. (B) Typical time course of M617-induced I_{Ba} inhibition in a neuron treated with VDCCs blockers. ω-CgTx GVIA (N-type VDCCs blocker, 1 μM) + ω-Aga IVA (P/Q-types VDCCs blocker, 1 μM) and M617 (10 μM) were bath-applied during the time indicated by the open and filled bars, respectively. (C) Typical superimposed I_{Ba} traces recorded using a double-pulse voltage protocol at the times indicated in the time course graph D. (D) Typical time course of M617-induced I_{Ba} inhibition in a neuron treated with VDCCs blockers. Nif (L-type VDCCs blocker, 10 μM) + ω-Aga IVA (P/Q-types VDCCs blocker, 1 μM) and M617 (10 μM) were bath-applied during the time indicated by the open and filled bars, respectively. (E) Fractional components of L-, N-, P/Q- and R-types I_{Ba} and those inhibited by M617 (10 μM). The total height of the bars (open and hatched) represents the mean ± SEM contribution of the indicated VDCCs type to the total I_{Ba}. The hatched bars represent the mean ± SEM inhibition by M617 of the corresponding VDCCs type. Numbers in parentheses indicate the number of neurons tested.

Fig.6 Current-voltage relations of distinct I_{Ba}. Each I_{Ba} were evoked by a series of voltage steps from a holding potential of −80 mV to test potentials between −80 and +40 mV in +10 mV increments in the absence (opened points) and presence (filled points) of 10 μM GAL. (A) Current-voltage relations of $I_{Ba\text{-}L(+R)}$ were obtained using a neuron treated with ω-conotoxin GVIA (ω-CgTx GVIA, N-type VDCCs blocker, 1 μM) and ω-agatoxin IVA (ω-Aga IVA, P/Q-types VDCCs blocker, 1 μM). (B) Current-voltage relations of $I_{Ba\text{-}N(+R)}$ were obtained using a neuron treated with Nifedipine (Nif, L-type VDCCs blocker, 10 μM) and ω-Aga IVA (1 μM). (C) Current-voltage relations of $I_{Ba\text{-}P/Q\,(+R)}$ were obtained using a neuron treated with Nif (10 μM) and ω-CgTx GVIA (1 μM). (D) Current-voltage relations $I_{Ba\text{-}R}$ were obtained using a neuron treated with Nif (10 μM), ω-CgTx GVIA (1 μM) and ω-Aga IVA (1 μM). Values of each I_{Ba} are the averages of five neurons.

Fig.1

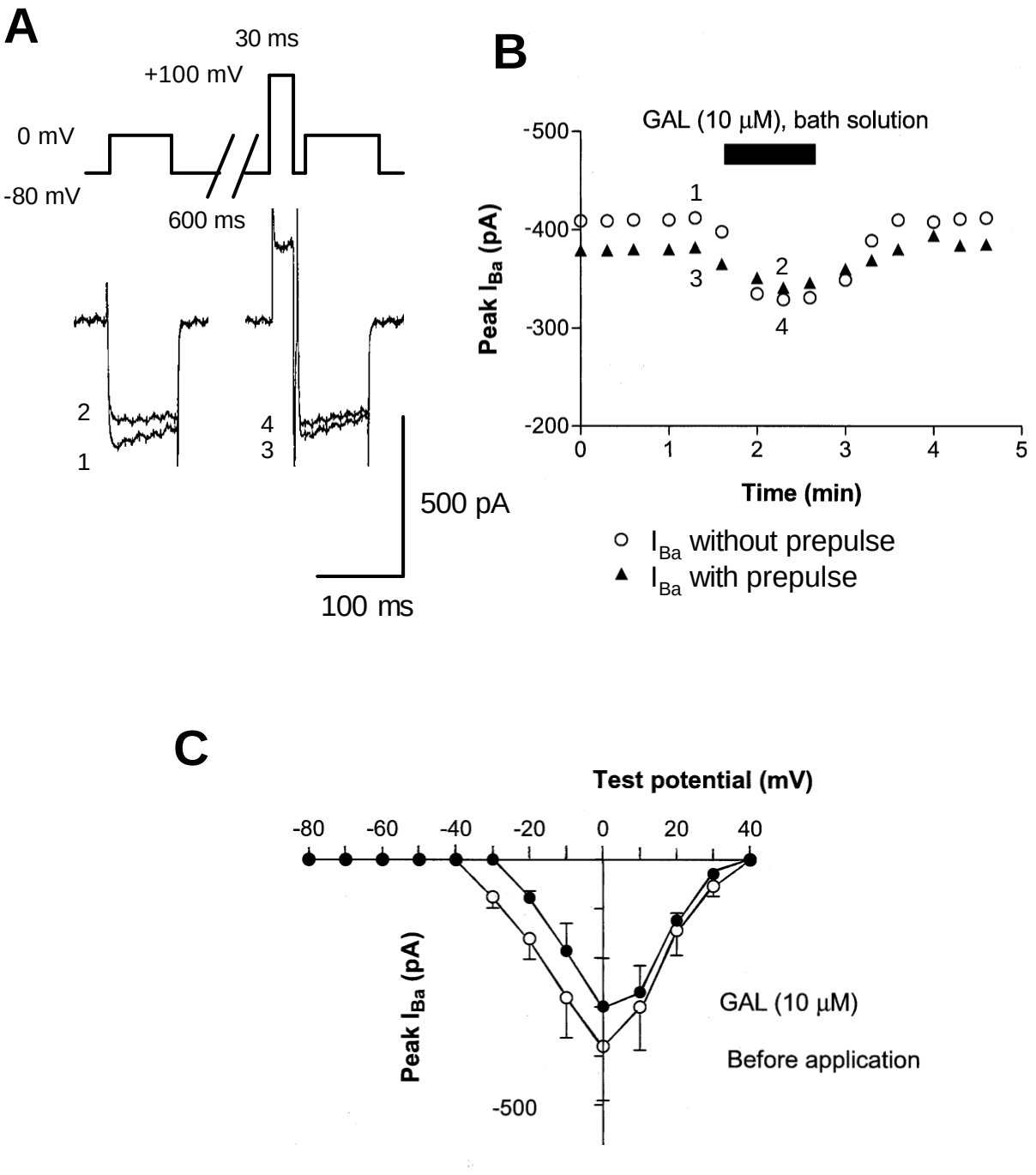
A
30 ms
+100 mV
0 mV
-80 mV
600 ms
2
1
4
3
500 pA
100 ms
B
GAL (10 μM), bath solution
Peak I_{Ba} (pA)
-500
-400
-300
-200
0
1
2
3
4
5
Time (min)
I_{Ba} without prepulse
I_{Ba} with prepulse
C
Test potential (mV)
-80
-60
-40
-20
0
20
40
Peak I_{Ba} (pA)
-500
GAL (10 μM)
Before application

Fig.2

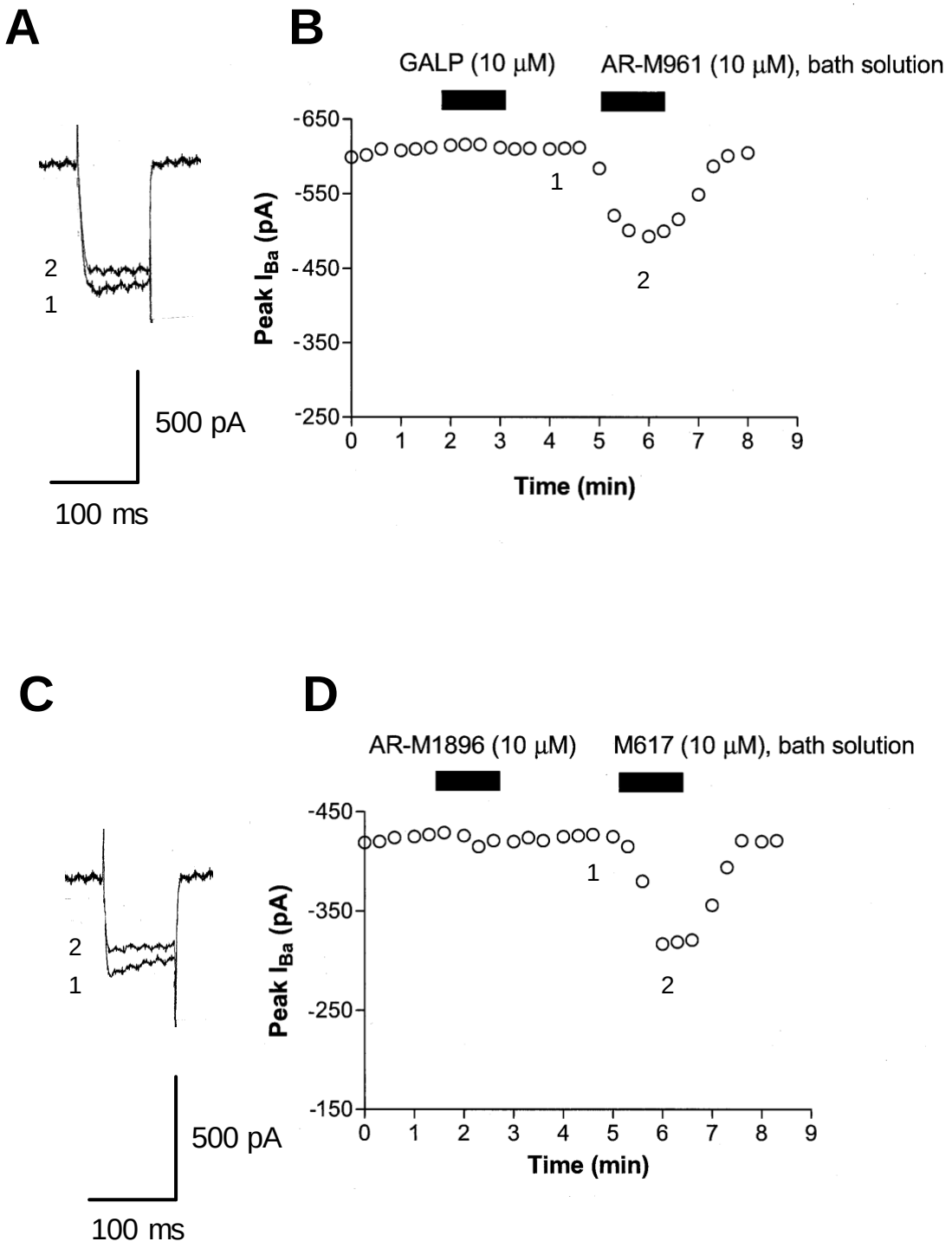
A
B
GALP (10 μM)
AR-M961 (10 μM), bath solution
2
1
500 pA
100 ms
Peak I_{Ba} (pA)
-650
-550
-450
-350
-250
0 1 2 3 4 5 6 7 8 9
Time (min)
C
D
AR-M1896 (10 μM)
M617 (10 μM), bath solution
-450
-350
-250
-150

Fig.3

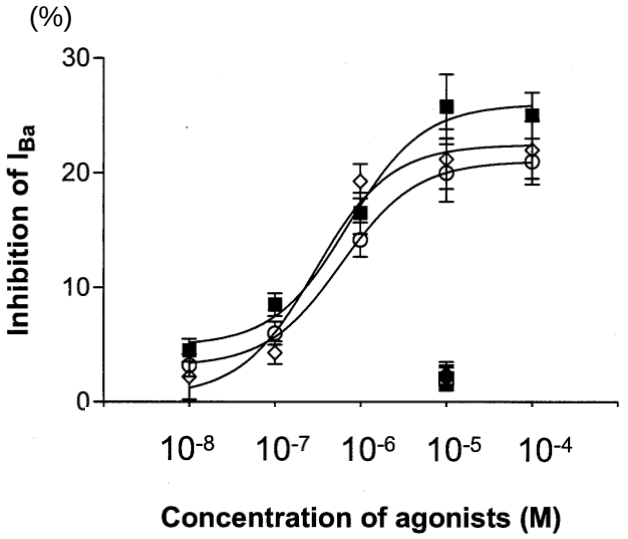

■ M617
○ GAL
◇ AR-M961
◆ Galanin(2-11)
● AR-M1896
□ GALP

Fig.4

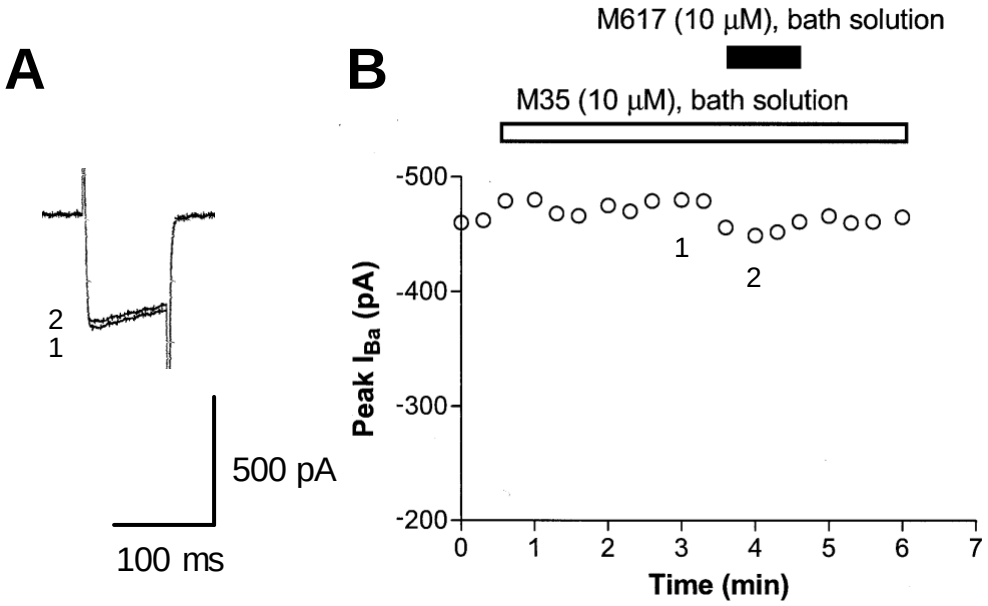
A
2
1
500 pA
100 ms
B
M617 (10 μM), bath solution
M35 (10 μM), bath solution
Peak I_{Ba} (pA)
-500
-400
-300
-200
1
2
0
1
2
3
4
5
6
7
Time (min)

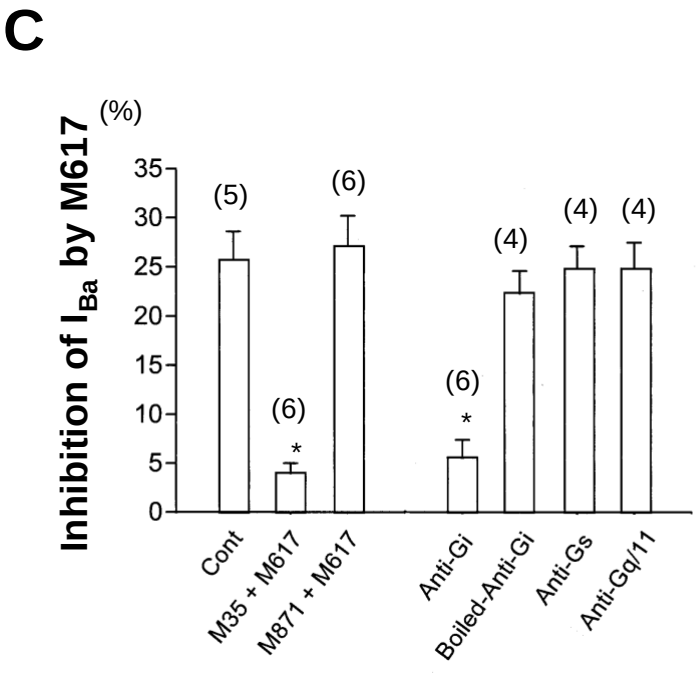
C
Inhibition of I_{Ba} by M617
(%)
35
30
25
20
15
10
5
0
(5)
(6)
(6)
*
(6)
*
(4)
(4)
(4)
Cont
M35 + M617
M871 + M617
Anti-Gi
Boiled-Anti-Gi
Anti-Gs
Anti-Gq/11

Fig.5

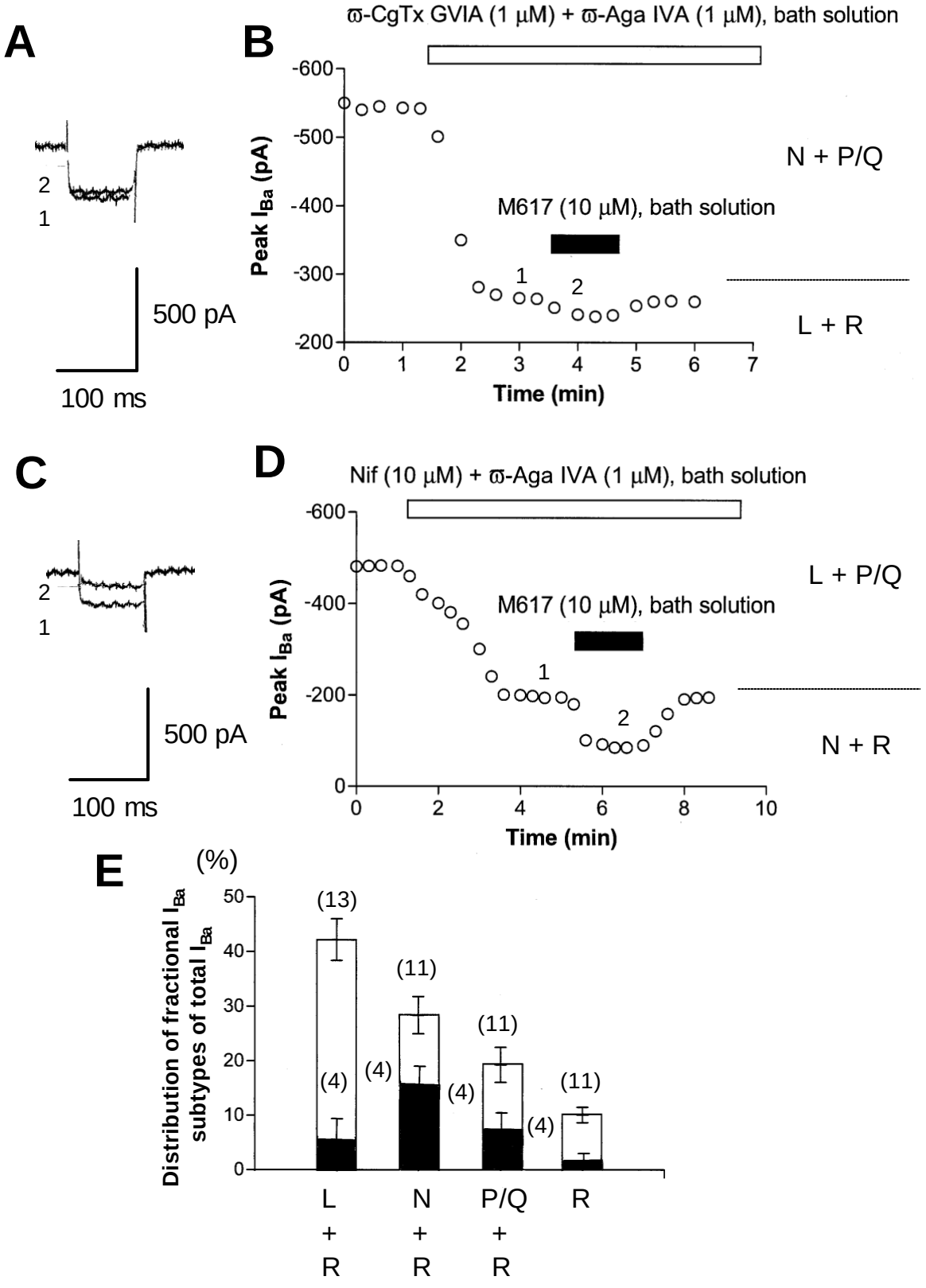
A
2
1
500 pA
100 ms
B
ϖ-CgTx GVIA (1 μM) + ϖ-Aga IVA (1 μM), bath solution
Peak I_{Ba} (pA)
-600
-500
-400
-300
-200
N + P/Q
M617 (10 μM), bath solution
1
2
L + R
0 1 2 3 4 5 6 7
Time (min)
C
2
1
500 pA
100 ms
D
Nif (10 μM) + ϖ-Aga IVA (1 μM), bath solution
Peak I_{Ba} (pA)
-600
-400
-200
0
L + P/Q
M617 (10 μM), bath solution
1
2
N + R
0 2 4 6 8 10
Time (min)
E
(%)
Distribution of fractional I_{Ba} subtypes of total I_{Ba}
50
40
30
20
10
0
(13)
(4)
(11)
(4)
(4)
(11)
(4)
(11)
L + R
N + R
P/Q + R
R

Fig.6

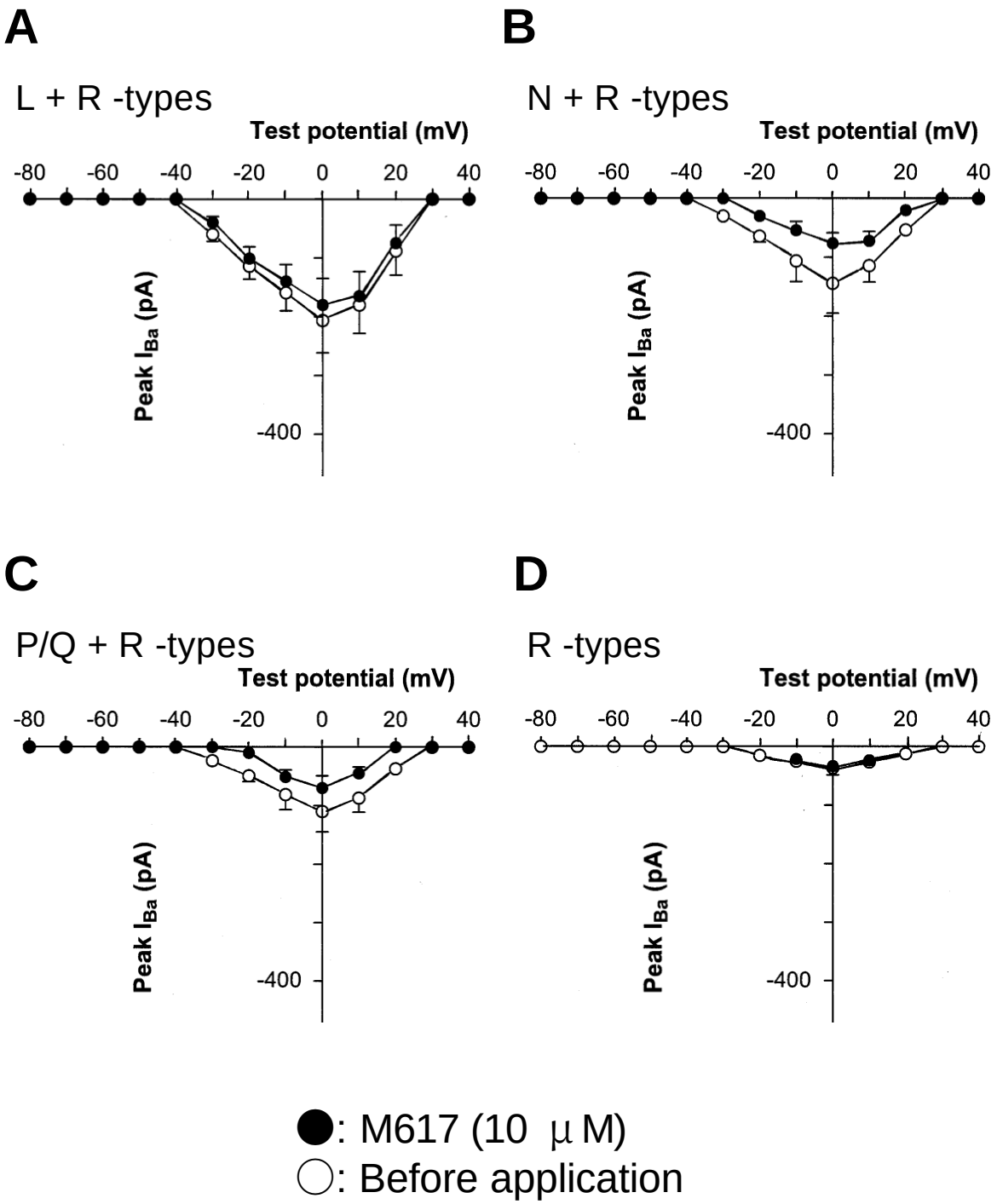
A
L + R -types
Test potential (mV)
-80 -60 -40 -20 0 20 40
Peak I_{Ba} (pA)
-400
B
N + R -types
Test potential (mV)
-80 -60 -40 -20 0 20 40
Peak I_{Ba} (pA)
-400
C
P/Q + R -types
Test potential (mV)
-80 -60 -40 -20 0 20 40
Peak I_{Ba} (pA)
-400
D
R -types
Test potential (mV)
-80 -60 -40 -20 0 20 40
Peak I_{Ba} (pA)
-400
●: M617 (10 μM)
○: Before application